

Rates and Equilibria for the Inactivation of Muscle Aldolase by an Active Site Directed Michael Reaction

Rossana Motiu-DeGrood, William Hunt, Joyce Wilde, and D. J. Hupe*

Contribution from the Department of Chemistry, The University of Michigan, Ann Arbor, Michigan 48109. Received October 3, 1978

Abstract: Compound **1**, 4-(4-nitrophenoxy)-2-keto-*n*-butylphosphoric acid, was synthesized and shown to undergo elimination of *p*-nitrophenol in aqueous solution at pH 7.0 to form 2-keto-3-butenylphosphoric acid (**2**) at a rate 50 times greater than hydration to 2-keto-4-hydroxybutylphosphoric acid (**4**) occurs. A term in the rate expression for $1^{2-} \rightarrow 2$ is ascribed to an intramolecular proton abstraction of the α proton by the phosphate oxygen. Rabbit muscle aldolase does not catalyze the production of even 1 equiv of *p*-nitrophenol in the presence of excess **1**. The elimination product, **2**, however, causes time-dependent inhibition of the enzyme. The pH and concentration dependence of this reaction was studied, as well as protection from inhibition by **2** using dihydroxyacetone phosphate. Formation of the mixed disulfide of β -mercaptoacetate with an active-site thiol group also affords protection from inhibition by **2**. The rate of hydrolysis of the enzyme-inhibitor complex was measured by two methods, and this demonstrated that the equilibrium constant for binding of **2** was 10^9 M^{-1} at pH 7. Compounds **1** and **4** were shown to bind to aldolase but not undergo reaction. A mechanism for inactivation is proposed in which **2** forms an iminium ion with the lysine function, followed by a Michael-type addition of a thiol to afford the inactive complex.

Introduction

We have previously shown¹ that 2-keto-3-butenylphosphate (**2**) inhibits rabbit muscle aldolase in an active site directed, time-dependent manner. A logical explanation of this behavior² is that **2** condenses with the ϵ -amino group of lysine present at the active site,³ followed by attack of an active-site nucleophile, as shown in Scheme I. The formation of the iminium ion would be analogous to the condensation of the natural substrate dihydroxyacetone phosphate (DHAP) with the enzyme. Aldolase does not catalyze the steady-state production of *p*-nitrophenol from **1**, even though a reasonable mechanism may be written using precedented reactions.⁴⁻⁷

In this paper we describe the details of the syntheses and reactivity of **1**, **2**, and **4** and their interactions with the enzyme. In particular, we wished to determine if a single turnover of **1** to **2** was catalyzed by aldolase and also to determine if the inhibition by **2** was reversible. It was also desirable to see if an active site directed thiol reagent would prevent inhibition in order to determine if a cysteine could be implicated as the reacting nucleophile.

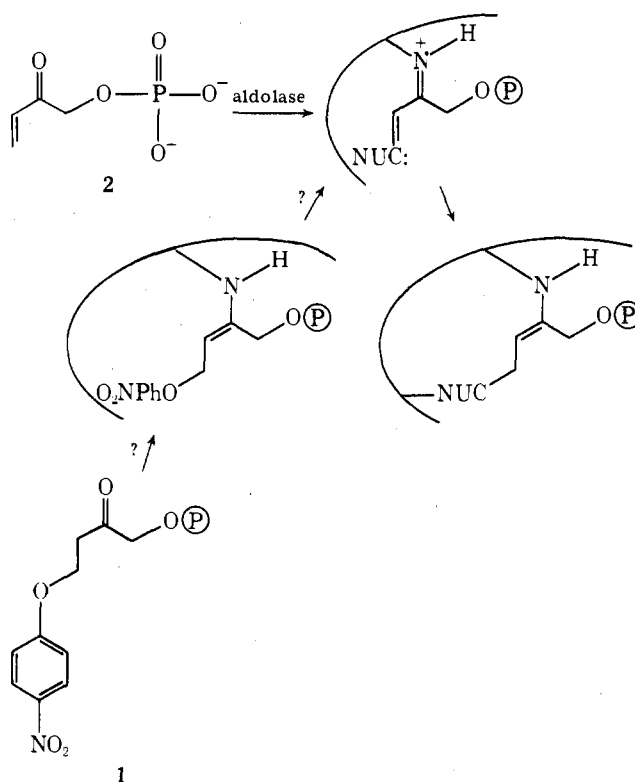
A study of both the forward and reverse rates of reaction might provide some generally useful information about the free energy of interaction covalent inhibitors with enzymes. Many of the suicide type of inhibitors or those that react further after a Michael-type reaction would not be amenable to study in both directions.^{8,9} An inhibitor of aldolase might also be practically useful in metabolic studies that required the disruption of glycolysis. In addition, the ability (or inability) of aldolase to catalyze an elimination reaction might give some insight into the stereochemistry of molecules bound to the active site.

Experimental Section

3-(4-Nitrophenoxy)propionyl Chloride (3b). In a typical synthesis, 5.2 g (0.025 mol) of 3-(4-nitrophenoxy)propionic acid (**3a**), prepared from *p*-nitrophenol and β -propiolactone, was dissolved in 300 mL of dry benzene, followed by the addition of 4.2 mL of oxalyl chloride (0.05 mol). The mixture was refluxed for 90 min during which time the evolution of gas ceased. The solvent and any other volatile components were removed under reduced pressure. Two 25-mL portions of ether were added and then removed under reduced pressure. The slightly yellow liquid thus obtained gave an NMR spectrum consistent with **3a** but was characterized no further: ¹H NMR (CDCl₃) δ 3.40 (t, 2 H), 4.33 (t, 2 H), 6.88 (d, 2 H), 8.05 (d, 2 H).

3-(4-Nitrophenoxy)-1-diazo-2-butanone (3c). The approximately 0.025 mol of **3b** prepared as described above was added to an ether

Scheme I



solution of approximately 0.1 mol of CH₂N₂ prepared by distillation. The solution was allowed to stir for 30 min at 0 °C and then solvent, excess CH₂N₂, and any other volatile materials were removed by a stream of N₂, creating an effluent stream which was passed through a trap of acetic acid in ether. There remained a solid which, when recrystallized from ether, yielded 4.45 g (0.0189 mol, 75% based on **3a**) of **3c**: mp 94–95 °C; IR 1750, 2130 cm⁻¹; ¹H NMR (CDCl₃) δ 2.83 (t, 2 H), 4.40 (t, 2 H), 5.40 (s, 1 H), 6.95 (d, 2 H), 7.84 (d, 2 H). Anal. Calcd for C₁₀H₉N₃O₄: C, 51.06; H, 3.86; N, 17.86. Found: C, 51.13; H, 4.00; N, 17.73.

4-(4-Nitrophenoxy)-2-keto-*n*-butylphosphoric Acid Monohydrate (1). A solution of 0.39 g (1.66 mmol) of **3c** in 100 mL of ether was added to a solution of 0.8 mL of 85% H₃PO₄ (11.7 mmol) in ether. This colorless homogeneous mixture was allowed to sit at 25 °C for 48 h during which time a spot due to **3c** on TLC (*R_f* 0.17, silica gel, ether) disappeared. The resulting solution was extracted with 3 × 10

mL portions of distilled water. The combined aqueous solutions were extracted with 2×5 mL of ether followed by passing a stream of N_2 through for several minutes. Aliquots of this solution did not instantly turn yellow when the pH was 8.0, but rapidly turned yellow when the pH was raised above 11.0. The intensity of this absorption in diluted aliquots allowed the estimation of the conversion to **1** from **3c**, which was close to 100%. The extinction coefficient for *p*-nitrophenoxide at 400 nm that was used in this calculation, 1.82×10^4 , was obtained from the average of six determinations done on carefully weighed samples of *p*-nitrophenol dissolved in water at pH 10. This value of ϵ agrees well with the literature value of 1.81×10^4 .¹¹

Solutions of **1** thus prepared were separated from phosphoric acid and any other impurities by chromatography on a Sephadex G-15 column (2.0 cm \times 25 cm). In a typical separation an amount of solution containing approximately 0.15 g of **1** (as determined by A_∞ measurements in NaOH solution) was loaded onto the column and eluted with distilled water. The fractions between 100 and 125 mL showed an intense yellow color when aliquots were added to NaOH solution, but no color when they were added to pH 7 buffer. These fractions were combined, frozen, and lyophilized to yield a white fluffy powder.

This material was purified to a high melting point by rechromatography in an identical manner. The rechromatographed material had an average molecular weight of 321 ± 3 , measured by *p*-nitrophenol production, which is consistent with the monohydrate. This procedure gives 65% yield from **3c** (50% overall yield from **3a**) of crystalline **1**·H₂O: mp 77–79 °C; IR (KBr) 1730 cm⁻¹; ¹H NMR (D₂O, pD 1.6) δ 3.11 (t, 2 H), 4.44 (t, 2 H), 4.65 (d, $J = 7.93$ Hz, 2 H, CH₂OP), 7.09 (d, 2 H), 8.23 (d, 2 H). Anal. Calcd for C₁₀H₁₄O₉NP: C, 37.16; H, 4.36; N, 4.33; P, 9.58. Found: C, 37.02; H, 4.30; N, 4.31; P, 9.55.

¹H NMR Studies on the Reaction of 1. The ¹H NMR spectra of a 0.02 M solution of **1** in D₂O were taken at various time intervals after adjusting the pD of the solution to 7.0. The spectra, shown in Figure 1, were measured on a JOEL 100-MHz Fourier transform NMR using a pulse technique to minimize the peak due to H₂O.

Preparation of Solutions of 2. The pH of a solution of **1** was raised to 7.5, and the slow generation of yellow color due to *p*-nitrophenoxide formation was allowed to occur for about 10 half-lives (15–20 h, 99.9% completed). The pH of the solution was lowered to 5.8 and the *p*-nitrophenol was removed by extraction with 3×10 mL portions of ether. A stream of N_2 was passed through this solution to remove any ether. The resulting solution of **2** had an absorbance maximum at 215 nm, as shown in Figure 1.

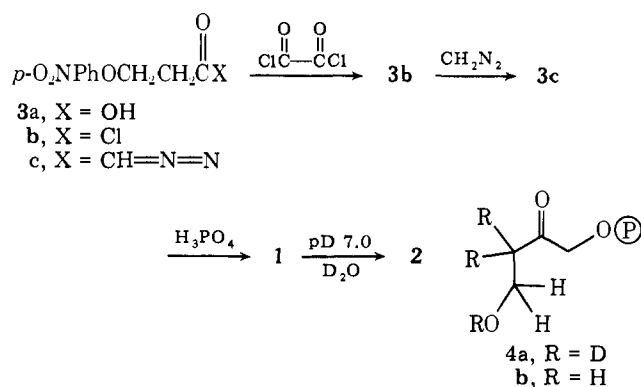
pH-Rate Profiles for 1 and 2. The rate of elimination of *p*-nitrophenol from **1** was monitored by measuring the appearance of *p*-nitrophenoxide ion at 400 nm on a GCA McPherson automated spectrophotometer at 25 °C. The concentration was chosen so that the A_∞ value was 10–25 upon addition of excess NaOH. The A_∞ under the conditions of the experiment was then calculated from the measured pH. The initial rate divided by the A_∞ value provided the k_{obsd} values used in Figure 2. The reactions were run in unbuffered solution by adjusting the pH with small amounts of NaOH. The pH values were measured before and after the rate measurements.

For those measurements at pH values below 6.0, the procedure was modified because of the very low rates and calculated A_∞ values. The initial rates were determined by diluting aliquots of the reaction mixture at specified times with pH 7, 0.001 M phosphate buffer and immediately measuring the *p*-nitrophenoxide present.

The rate of hydration of **2** to **4b** in unbuffered aqueous solution at a given pH value was determined by measuring the disappearance of **2** at 215 nm at 25 °C. Since the reactions were slow, the absorbance readings were made by measuring the spectra of aliquots of reaction mixture taken from a sample thermostated at 25 °C. The pH of each run was measured at various time intervals. The rate constant for the reaction of 4-(4-nitrophenoxy)-2-butanone with phosphate dianion was determined by measuring the rate of production of *p*-nitrophenoxide as described previously.¹² The rates were measured for eight concentrations of phosphate at each of three pH values, 8.5, 7.2, and 6.2. The observed rate constants were plotted vs. the concentration of phosphate dianion, which was computed from the total phosphate concentration and the measured pK_a^2 of phosphate, 6.48. The slopes of the lines through the points were independent of pH and had a value of $k = 3.5 \times 10^{-4} \text{ M}^{-1} \text{ s}^{-1}$.

Preparation of Enzyme and Measurement of Activity. Rabbit muscle aldolase was purchased from Calbiochem and desalted by passing a

Scheme II



1:10 dilution of the enzyme suspension through a 2×10 cm G-25 Sephadex column, and collecting the fractions immediately following the void volume. The concentration of enzyme in this preparation was determined by measuring the absorbance at 280 nm, using $\epsilon_{280}^{1\%} = 9.38$.¹³ The activity of the enzyme in a sample was determined by adding 0.050 mL of the solution to 0.750 mL of an assay mixture obtained from Calbiochem containing 2.0×10^{-4} M NADH, 4.3×10^{-3} M fructose 1,6-bisphosphate, α -glycerolphosphate dehydrogenase, and triosephosphate isomerase buffered at pH 7.0. The activity was monitored by measuring the rate of loss of absorbance at 340 nm at 37 °C. Control studies showed that the presence of **2** in the assay mixture did not change the measured aldolase activity. Also, the plots of the absorbance vs. time were linear with or without **2** present.

In most of the studies described below, an incubation mixture was prepared containing buffer, water, and other appropriate reagents and then the mixture was equilibrated in a constant temperature bath before addition of an aliquot of enzyme at $t = 0$. At specified times, 0.050-mL samples of the incubation mixture were added to 0.750-mL portions of assay mixture in cuvettes that were held at 37 °C. Usually four or more of these measurements were made in order to determine the rate of inactivation under a given set of conditions.

The measurement of the rate of reaction of **2** with aldolase in the presence of various concentrations of **1** required special precautions because of the significant production of **2** from **1** during the course of an experiment in buffered solution. A solution of 1.25×10^{-3} M **1** was prepared at pH 3.5 and this was kept at 0 °C to minimize conversion to **2**. Also prepared were a solution of 1.3×10^{-3} M **2** adjusted to pH 7.0, a stock solution of enzyme, also at pH 7.0, and a stock 10^{-4} M imidazolium acetate buffer solution, also adjusted to pH 7.0. The pH of an aliquot of **1** was adjusted to 7.0 just prior to use. A 300- μ L sample of the solution of **1** (or a lesser amount diluted to 300 μ L with water) was transferred to a vial thermostated at 37 °C, which also contained 50 μ L of **2** and 50 μ L of buffer. After temperature equilibration was achieved, 100 μ L of enzyme previously warmed to 37 °C was added. After 35 s, 50 μ L of the incubation mixture was added in the usual manner. A parallel control experiment, using water instead of the solution of **2**, was performed at the same time.

A control experiment was performed in which **1**, water, and buffer were mixed in concentrations comparable to those used in the other measurements. After allowing the same amount of time to elapse, at the same temperature, the amount of *p*-nitrophenol produced was measured spectrophotometrically. This showed that during the course of the experiments described above, approximately 25% of the **1** initially used had been converted to **2** and *p*-nitrophenol.

Results

Synthesis and Reactivity of 1, 2, and 4. The synthesis of compound **1** was accomplished as is shown in Scheme II in 50% overall yield from the known¹⁰ acid **3a**. Compound **1** was obtained as a crystalline solid monohydrate, as determined from both elemental analysis and the absorbance of *p*-nitrophenoxide obtained upon treatment with base. The NMR spectrum of **1**, shown in Figure 1, initially changes only slightly when the pH is raised from 1.7 to 7.0, but then changes to a spectrum consistent with the structure of **2** in about 24 h. A slower change occurs over the next 10 days, which produces a spectrum consistent with **4a**, in which hydration of the

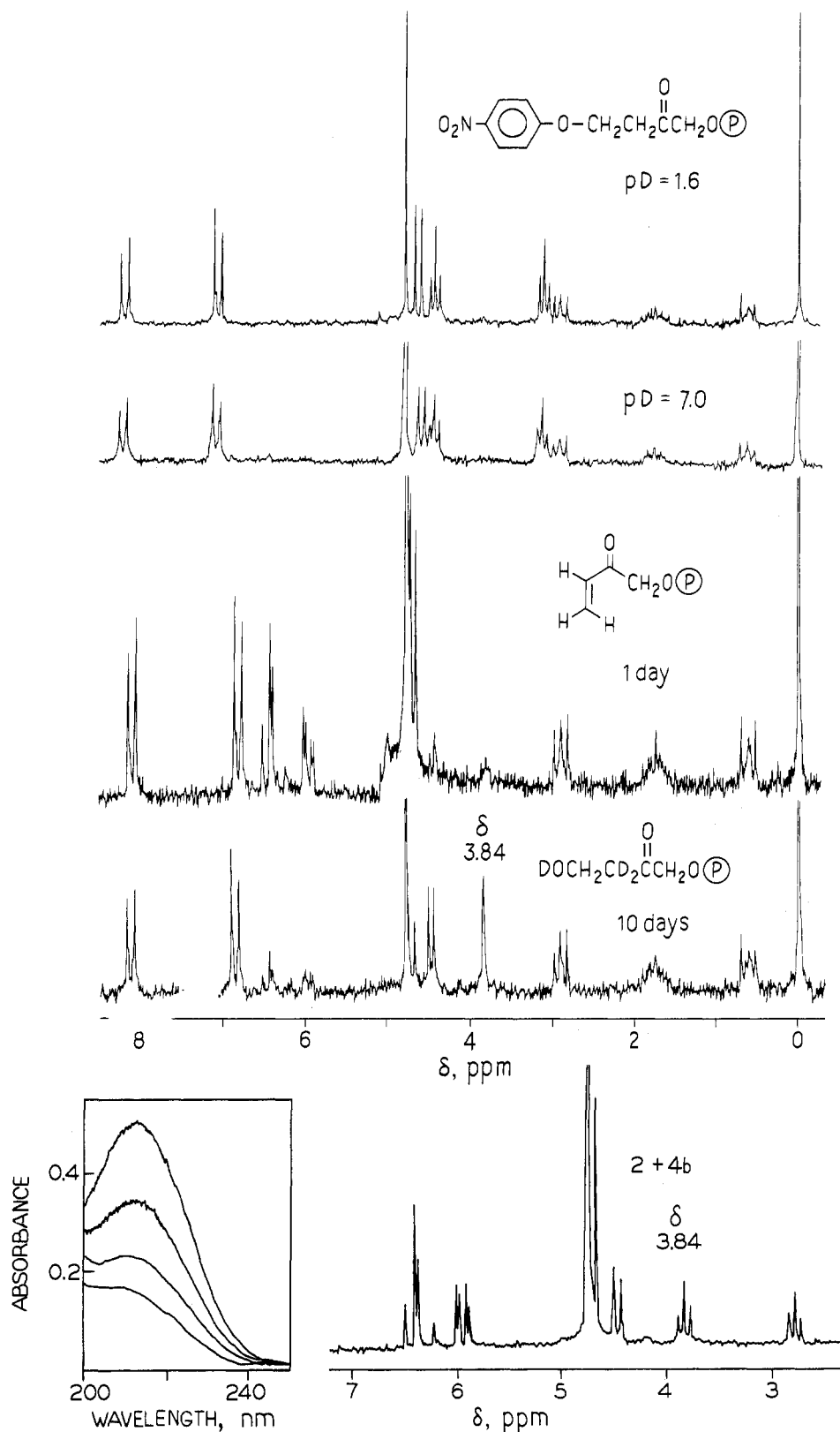


Figure 1. The top spectrum is that for 10^{-2} M **1** in D_2O at $\text{pD} 1.6$, and the spectrum just below is the same sample raised to $\text{pD} 7.0$. After 1 day, a spectrum consistent with **2** appears, which then converts to that for **4a** after 10 days. The peaks at $\delta 0.7, 1.8,$ and 2.9 are due to the 3-(trimethylsilyl)-1-propanesulfonic acid used as a standard. On the lower right is a spectrum of a mixture of **4b** and **2**, which was prepared in H_2O . The spectrum was taken immediately after exchanging the solvent for D_2O . On the lower left is shown a UV spectrum of **2** with λ_{max} at 215 nm, which slowly diminishes as **2** is converted to **4b**.

enone¹⁴ and α -deuterium exchange¹⁵ have occurred. This assignment was confirmed by creating a solution of **4b** in H_2O by essentially the same method and then replacing the solvent with D_2O , as is also shown in Figure 1.

Solutions of **2** were prepared by allowing solutions of **1** to

stand at room temperature for 20 h, followed by extraction of *p*-nitrophenol. The absorbance spectrum of **2** showed a characteristic¹⁴ peak at 215 nm, which slowly disappeared as **2** was converted to **4**.

As shown in Figure 2, the pH-rate profile for the conversion

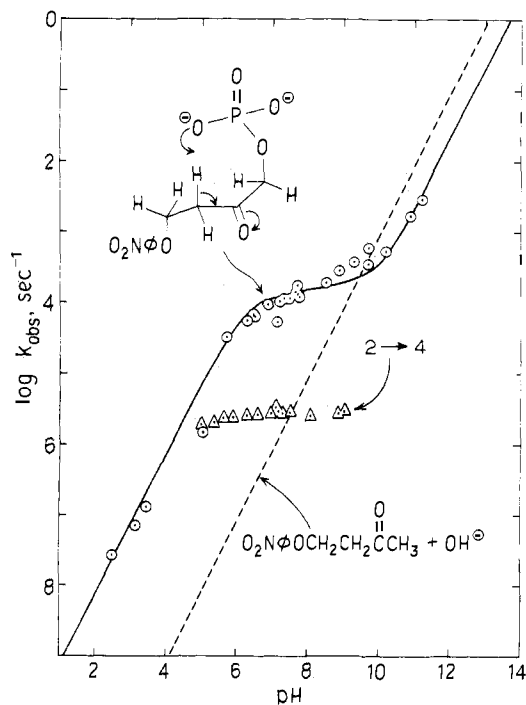


Figure 2. The circles are measured points on a pH-rate profile for production of *p*-nitrophenol from **1**, which is fit by a line computed using $k_{\text{obsd}} = k_1[\text{I}^{2-}] + k_2[\text{OH}^-][\text{I}^{2-}]$, where $k_1 = 1.30 \times 10^{-4} \text{ s}^{-1}$ and $k_2 = 2.13 \text{ M}^{-1} \text{ s}^{-1}$. A value of $\text{p}K_a(\text{ROPO}_3\text{H}^-) = 6.80$ was used for the computation. The dashed line represents the pH-rate profile for 4-(4-nitrophenoxy)-2-butanone. The term proportional to the dianion of **1** is ascribed to an intramolecular proton abstraction as shown. The triangles define a pH-rate profile for the conversion of **2** to **4**, which is pH independent at neutral pH with a rate constant of $2.5 \times 10^{-6} \text{ s}^{-1}$. At neutral pH, where the changes shown in Figure 1 occur, the rate constant for the conversion of **1** to **2** is about 50 times greater than the rate of conversion of **2** to **4**. This accounts for the ability to cleanly generate solutions of metastable **2** under these conditions.

of **1** to **2** was different than that obtained for 4-(4-nitrophenoxy)-2-butanone (**5**), a compound that is identical with **1** but without the phosphate group.¹² The rate law for **5** was shown to be $v = 8.3 \text{ M}^{-1} \text{ s}^{-1} \times [\text{5}][\text{OH}^-]$, whereas that used to compute the solid line in Figure 2 for **1** was $v = 2.13 \text{ M}^{-1} \text{ s}^{-1} \times [\text{I}^{2-}][\text{OH}^-] + 1.30 \times 10^{-4} \text{ s}^{-1} \times [\text{I}^{2-}]$. The $\text{p}K_a^2$ of **1** used to calculate the concentration of $[\text{I}^{2-}]$ from the total concentration of **1** was 6.80, which is comparable to $\text{p}K_a^2$ values for other α -ketophosphates.

The pH-rate profile for the conversion of **2** to **3** is also shown in Figure 2. The rate is roughly independent of pH with a rate constant of $2.5 \times 10^{-6} \text{ s}^{-1}$. The fact that clean aqueous solutions of **2** may be generated from **1** reflects the fact that at pH 7.0 the conversion of **1** to **2** occurs about 50 times faster than the conversion of **2** to **4**. By using these known rates and the integrated rate expression for the conversion of $\text{A} \rightarrow \text{B} \rightarrow \text{C}$, a correction may be made for the small amount of **2** that is converted to **4** during the synthesis of **2** from **1** at pH 7.0. This allows a corrected extinction coefficient of 6.5×10^4 ($\lambda_{\text{max}} 215 \text{ nm}$) to be calculated for **2**.

A rate constant of $3.5 \times 10^{-4} \text{ M}^{-1} \text{ s}^{-1}$ was measured for the reaction of 4-(4-nitrophenoxy)-2-butanone with phosphate dianion using previously described methods.¹²

Aldolase and 1. A number of unsuccessful attempts were made to observe aldolase-dependent production of *p*-nitrophenol from **1**. For example, 1.5 mL of a solution of $1.51 \times 10^{-4} \text{ M}$ **1**, having an absorbance of 0.201 at 400 nm, was mixed rapidly¹⁶ with 1.0 mL of a solution of $1.9 \times 10^{-5} \text{ M}$ aldolase. A decrease in absorbance to 0.120 occurred which was exactly the amount expected for dilution. An increase in absorbance of 0.070 would have been observed at this pH if one *p*-nitro-

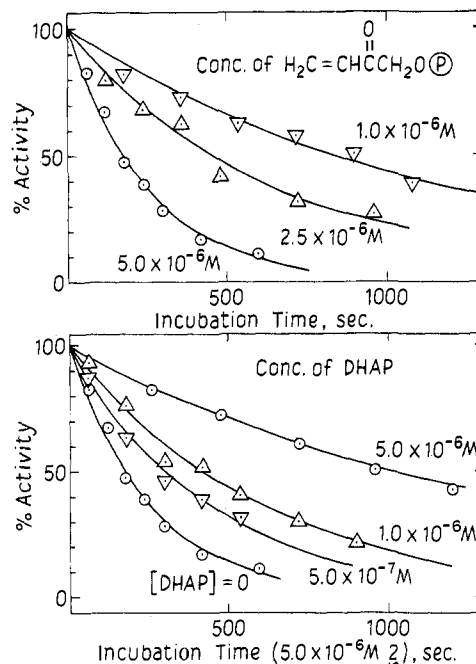


Figure 3. The upper plot shows the dependence of the percent inactivation on the concentration of **2** and the length of the incubation time. The lower plot demonstrates the protection afforded aldolase by various concentrations of DHAP. The K_m for DHAP, computed as described in the text, was $1.4 \times 10^{-6} \text{ M}$. These data were obtained at pH 7.0 in unbuffered solution and are similar to data obtained in 10^{-4} M imidazolium acetate buffer at the same pH value.

phenol per enzyme molecule had been produced. The slopes of plots of absorbance vs. time for the conversion of **1** to **2** plus *p*-nitrophenol were identical before and after addition of enzyme, indicating that no enzyme-catalyzed steady-state production of *p*-nitrophenol was occurring.

Inhibition of Aldolase by 2. In Figure 3 are data showing that incubation of aldolase with **2** in low concentrations causes time-dependent inhibition. Whereas the data in Figure 3 were obtained in unbuffered solution, essentially identical rate constants were measured in the presence of 10^{-4} M imidazolium acetate buffer. As shown in Figure 4, the rate of inhibition measured at low concentrations of **2** is pH dependent and exhibits a maximum near pH 7.0. The k_{obsd} values for inactivation achieve saturation at high concentrations of **2**, as is also shown in Figure 4.

If it is assumed that the enzyme forms a dissociable complex $\text{E} \cdots \text{2}$, which then converts to a stable adduct $\text{E}-\text{2}$ (irreversible under the conditions studied), then the appropriate expression¹⁷ for describing the rate of inhibition is shown in eq 1. The quantity $k_{\text{obsd}}^{\text{max}}$ is the observed rate constant at infinite concentration of **2** and K_2^i is the dissociation constant for $\text{E} \cdots \text{2}$. Equation 1 was used to calculate the solid line in Figure 3 using $K_2^i = 9.9 \times 10^{-5} \text{ M}$ and $k_{\text{obsd}}^{\text{max}} = 1.12 \times 10^{-1} \text{ s}^{-1}$.

$$\text{E} + \text{2} \xrightleftharpoons[k_{-1}]{k_1} \text{E} \cdots \text{2} \xrightleftharpoons[k_{-2}]{k_2} \text{E}-\text{2}$$

$$\frac{1}{k_{\text{obsd}}} = \frac{K_2^i}{k_{\text{obsd}}^{\text{max}}[\text{2}]} + \frac{1}{k_{\text{obsd}}^{\text{max}}} \quad (1)$$

All of the data above were obtained under conditions where the concentration of **2** is at least 100 times greater than the concentration of the enzyme, as determined from absorbance measurements at 280 nm using $\epsilon_{280}^{1\%} = 9.38^{13}$ and mol wt 160 000.¹⁸ As is shown in Figure 5, with a concentration of **2** of $1.0 \times 10^{-5} \text{ M}$, the measured value of k_{obsd} drops rapidly when the concentration of enzyme exceeds 10^{-7} M . This is consistent with depletion of **2** from solution by reaction with the 16 exposed thiol groups present on native aldolase,¹⁸ which

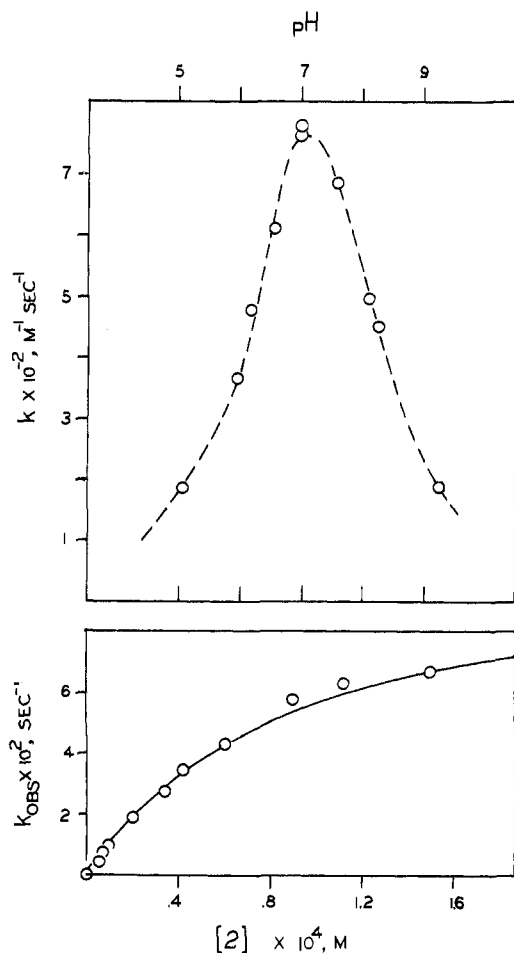


Figure 4. The upper plot shows a pH-rate profile for the reaction of 1.26×10^{-5} M **2** with aldolase at 37°C . Each point was determined from at least four activity measurements on incubation mixtures maintained at the pH shown using 10^{-4} M imidazolium acetate buffer. Below is a plot of similarly measured k_{obsd} values as a function of concentration of **2**, which show saturation at high concentrations of **2**. The solid line was computed as described in the text using $k_{\text{obsd}}^{\text{max}} = 1.12 \times 10^{-1} \text{ s}^{-1}$ and $K_2^i = 9.9 \times 10^{-5}$ M.

have been shown previously to react readily with oxidizing^{19,20} and alkylating²¹ agents.

Protection from Inhibition. If **2** is an active site directed inhibitor which causes a loss of activity that is irreversible under the conditions studied, then protection from inhibition should occur upon addition of a reversible inhibitor, **I**. The rate of inactivation by **2** in the presence of **I** is governed by eq 2:¹⁷

$$\frac{1}{k_{\text{obsd}}} = \frac{K_2^i}{k_{\text{obsd}}^{\text{max}}[\mathbf{2}]} \left(1 + \frac{[\mathbf{I}]}{K^i} \right) + \frac{1}{k_{\text{obsd}}^{\text{max}}} \quad (2)$$

In this expression **[I]** is the concentration of reversible inhibitor added and K^i is the corresponding dissociation constant for the complex formed by **I** and the enzyme.

In Figure 3 are shown data for the reaction of **2** with aldolase in the presence of various concentrations of dihydroxyacetone phosphate (DHAP). The value of K^i ($=K_m$) for DHAP was determined from a plot of $1/k_{\text{obsd}}$ vs. **[DHAP]**, which had a slope of $K_2^i/k_{\text{obsd}}^{\text{max}}[\mathbf{2}]K^i$. The value of K^i for DHAP obtained by this method is 1.4×10^{-6} M, which is smaller than the literature value of 4.5×10^{-6} M that was measured by fluorescence quenching.²² Since that value was determined in the presence of chloride ion, a reversible inhibitor for aldolase, these values are consistent.

In order to determine whether **1** or **4** binds to the enzyme, similar sets of experiments were done in which the rate reaction

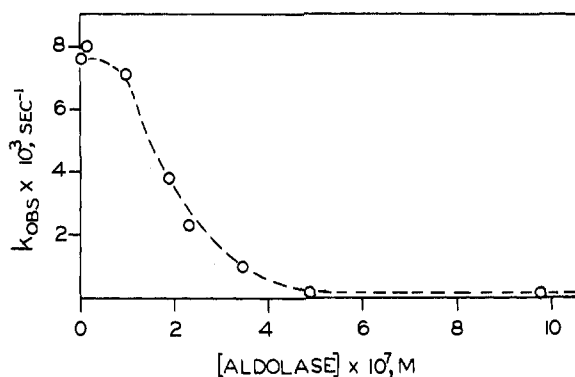


Figure 5. A plot of the rate constants for inactivation of aldolase by 1.0×10^{-5} M **2** as a function of the concentration of the enzyme used. At **[2]/[aldolase]** ratios of less than 100, the apparent rate constant decreases. For this reason all of the data described in this study were done with an enzyme concentration less than 1/100th that of the lowest concentration of **2** that was used. This behavior is consistent with the depletion of **2** by reaction with the 16 non-active-site thiol groups previously shown to be susceptible to alkylation.

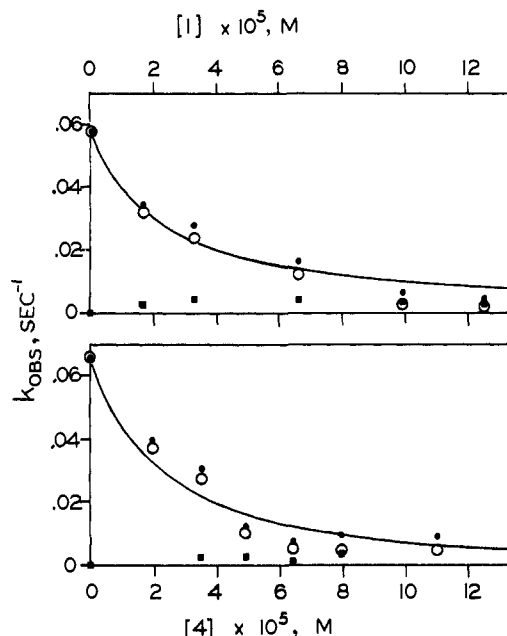


Figure 6. In the upper plot is shown the dependence of the observed rate for inactivation by **2** in the presence of varying concentrations of **1**. The background k_{obsd} value for inactivation by **1** without added **2** (■) was subtracted from the k_{obsd} value measured in the presence of **1** and **2** (●) to give a corrected value (○). They are fit by a line generated with eq 2 by using $K_2^i = 8 \times 10^{-6}$ M. A comparable experiment is shown in the lower plot in which binding by **4** prevents inhibition by 1.3×10^{-5} M **2**. The value of $K_4^i = 7 \times 10^{-6}$ M.

of **2** with aldolase was measured in the presence of various concentrations of **1** and **4**. Because **2** is generated rapidly from **1** and because **2** was present in small quantities in the samples of **4** used, it was necessary to perform control experiments simultaneously, so that the rate of inhibition due to the solution of **1** or **4** could be subtracted from the larger rate due to the known concentration of **2** that had been added. As shown in Figure 6, the presence of small concentrations of **1** or **4** successfully inhibits the reaction of aldolase with **2**. Using eq 2, an apparent dissociation constant of 8.3×10^{-6} M for the complex of aldolase with **1** was determined, along with a comparable value of 7.4×10^{-6} M for **4**.

Horecker had previously shown that a thiol at the active site of aldolase reacts with carboxyethyl disulfide to form a mixed disulfide causing inactivation, which is readily reversed upon

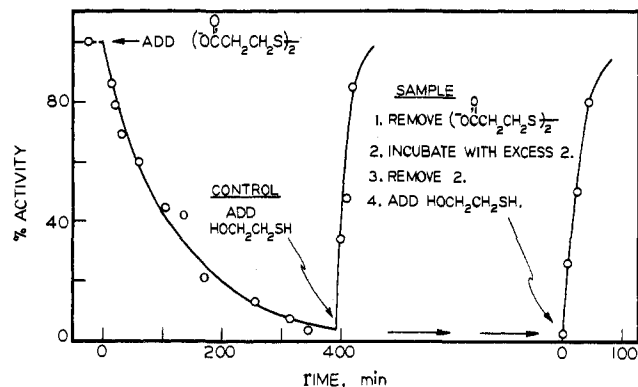


Figure 7. This plot shows the time-dependent disappearance of activity, which is caused by incubation with 0.025 M carboxyethyl disulfide, and the rapid regeneration of activity caused by addition of 0.35 M mercaptoethanol. Incubation of the treated enzyme with **2** does not result in activation which is irreversible (on this time scale). This is consistent with the formation of an active-site disulfide which protects the enzyme from reaction with **2**.

addition of mercaptoethanol.²¹ In Figure 7 is shown a similar experiment in which the activity of a sample of the enzyme is diminished by treatment with 0.025 M carboxyethyl disulfide at pH 7.9. An aliquot of this material treated with mercaptoethanol rapidly regains activity, as previously described.²¹ Another aliquot, after separation from excess carboxyethyl disulfide by gel filtration, was treated with an excess of **2** for several hours. Native aldolase would have been inactivated completely in several minutes under these conditions. After removal of excess **2** by gel filtration, rapid activation of the enzyme occurs upon addition of mercaptoethanol. (This activation is several orders of magnitude faster than the reactivation of E-2 in the presence of mercaptoethanol described below.)

Reversal of Inhibition. On a 50.0 × 2.5 cm Sephadex G-25 column eluted with 10⁻⁴ M imidazolium acetate buffer, aldolase, as measured either by activity or by absorbance at 280 nm, is eluted near the void volume, as shown in Figure 8. After inhibition with **2**, the absorbance due to the inactive protein elutes at the same point, although the activity has, of course, disappeared. The excess enone present could not be measured by ultraviolet spectroscopy because of the interfering absorbance of the imidazolium acetate buffer. Aliquots of the fractions around 200 mL, however, did show inhibitory ability, indicating the position of elution of **2**. In an identical column eluted with water instead of buffer, the absorbance due to **2** at 215 nm did elute at this same volume.

It seemed reasonable to expect, therefore, that if E-2 were to hydrolyze to E and **2** during a passage through the column, separation would occur and active enzyme would be generated. As shown in Figure 9, when samples of enzyme inhibited to a low fraction of activity were passed through the column, the activity per unit of protein increased. After several passages, substantial activity had been regenerated. These experiments were done at 25 °C rather than 37 °C to prevent loss of activity due to denaturation, which was shown to be negligible in a control experiment under identical conditions. The rate of regeneration of activity was determined at three different pH values, as shown in Figure 9, and this appears to be roughly independent of pH, in contrast to the forward reaction.

In a separate experiment, a sample of E-2 was incubated with a high concentration of mercaptoethanol on the presumption that if the same hydrolysis occurred, the **2** that was produced would be rapidly trapped by a Michael reaction. A control experiment showed that no substantial amount of activity was lost by native aldolase during similar treatment. The rate of regeneration of enzyme measured by this technique

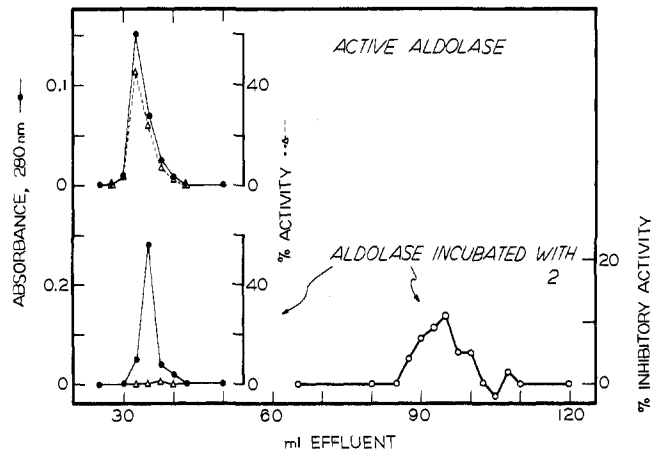


Figure 8. As shown in the upper plot, aldolase activity and absorbance at 280 nm elute at the same volume, which is close to the void volume of the 2.5 × 50 cm Sephadex G-15 column used with 10⁻⁴ M imidazolium acetate buffer adjusted to pH 7.0 as the eluent. After inactivation with **2**, the protein appears at the same volume, whereas the unreacted **2** appears much later. The presence of **2** was determined by measuring the ability of aliquots of eluent to inactivate aldolase.

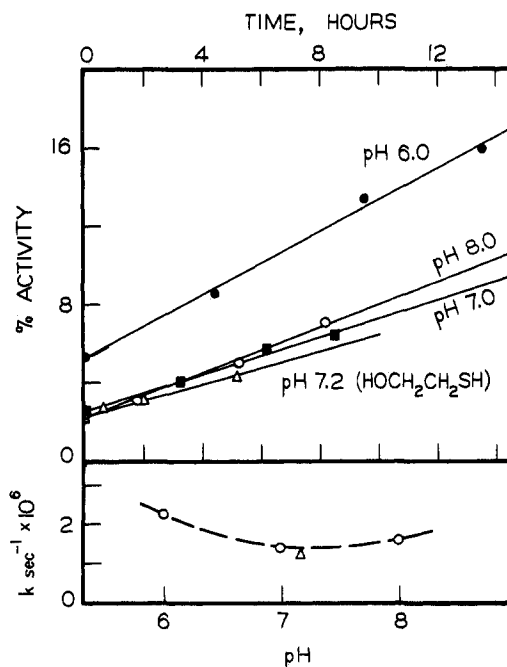


Figure 9. Samples of aldolase were treated with **2**, so that only a small fraction of their activity remained, and then were placed on a 2.5 × 50 cm Sephadex G-15 column maintained at 25 °C. The pH during inactivation and the several hours of elution time were maintained with a 10⁻⁴ M imidazolium acetate buffer adjusted to the indicated pH value. The activity of the eluted protein was measured and corrections for dilution were based on the absorbance at 280 nm. The increase in activity measured was followed by further increases obtained after chromatographing again for the length of time shown. The rate constant for reactivation at each pH value was obtained from the slope of these plots, and appeared to be roughly constant throughout the range 6–8. A similar rate constant for reactivation at pH 7.2 was obtained without resorting to chromatography by simply adding 0.35 M mercaptoethanol.

corresponds closely to the value measured by the multiple gel-filtration method described above.

Discussion

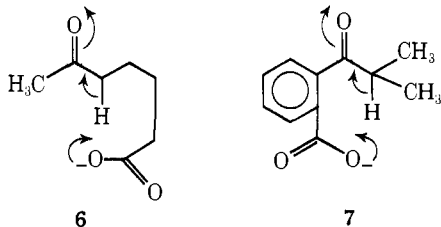
The fact that a first-order term proportional to the concentration of the dianion of **1** appears in the rate expression for production of *p*-nitrophenol from this substance suggests that an intramolecular proton transfer is occurring. Since the

Table I. Binding and Rate Constants for Aldolase and $\text{RC}(=\text{O})\text{CH}_2\text{O}^\ominus$

R	K_m or K_i	$k_{\text{obsd}}^{\text{max}}$, s^{-1}
HOCH_2	1.4×10^{-6}	
$\text{O}_2\text{NPhOCH}_2\text{CH}_2$	8×10^{-6}	
HOCH_2CH_2	7×10^{-6}	
ICH_2^a	4.3×10^{-4}	0.13
$\text{H}_2\text{C}=\text{CH}$	9.9×10^{-5}	0.112

^a Data taken from ref 20.

rate-determining step for this type of elimination reaction is proton transfer,¹² the first-order rate constant measured, $1.30 \times 10^{-4} \text{ s}^{-1}$, may be compared with an appropriate second-order process to obtain an "effective molarity" of the phosphate dianion in the transition state.²³ The second-order rate constant for the reaction of 4-(4-nitrophenoxy)-2-butanone with phosphate dianion is $3.5 \times 10^{-4} \text{ M}^{-1} \text{ s}^{-1}$, leading to a value of 0.4 M for the effective molarity of the intramolecular process. This value is comparable to other examples of intramolecularly catalyzed proton transfer from carbon, which are generally in the range of 10^{-1} to 10^2 M . For example, the intramolecularly catalyzed proton abstraction reaction of 7-ketooctanoate (**6**), which has a seven-membered transition

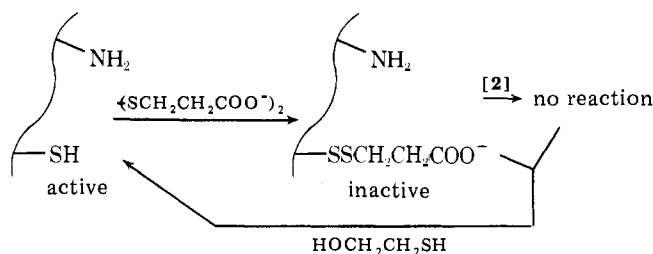


state like **1**²⁻, exhibits an effective molarity of 0.05 M,²⁴ whereas that calculated for **7** has a value of 50 M.²⁵ A value of 0.4 M is therefore reasonable for **1**²⁻.²⁰ This provides a good model for the previously postulated intramolecular mechanism²⁶ for aldolase itself, in which the phosphate group is responsible for the abstraction of the α proton from the iminium ion formed with lysine. This mechanism would explain the finding that dihydroxyacetone sulfate is bound to aldolase like DHAP, but does not undergo α -proton abstraction or subsequent condensation.²⁷ Since the oxygens of the sulfate derivative are much less basic than the corresponding oxygens of the phosphate analogue, intramolecular proton abstraction would be ineffective.

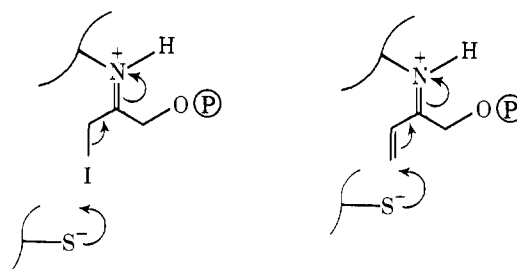
The rate of hydration of **2** to **4** is relatively independent of pH and about 50 times slower than the conversion of **1** to **2** at neutral pH values, so that solutions of this metastable compound may be made easily. Most, but not all,²⁸ Michael-type covalent enzyme inhibitors are so reactive that their generation at the active site using suicide inhibitors is required.² Vinyl glycolate has been oxidized in situ in order to produce a solution of a reactive enone similar to **2**, which acts as an inhibitor of the phosphotransferase system.²⁹ The existence of this substance was inferred from chemical behavior rather than by generation of the pure material. The fact that solutions of **2** can be prepared cleanly offers an opportunity for the quantitative study of the rates and equilibria involved in the interaction of this type of active site directed, Michael-type inhibitor with an enzyme.

The time-dependent inhibition of aldolase by **2** is prevented by the addition of the natural substrate DHAP, indicating that attack occurs at the active site. A saturation curve, typical for "irreversible" inhibitors, indicates that the binding is followed by conversion to the stable adduct E-**2** (with $k_{\text{obsd}}^{\text{max}} = 1.12 \times 10^{-1} \text{ s}^{-1}$).

Table I demonstrates an interesting similarity between the

Scheme III

rate data for **2** and those for α -iodoacetol phosphate, a compound which Hartman has shown to be a time-dependent active site directed inhibitor for aldolase.^{19,20} This inhibitor acts by oxidizing an active-site thiol group, presumably by first forming a sulfenyl iodide. The corresponding α -bromo and α -chloro analogues do not inactivate the enzyme by oxidation (or by alkylation). This is consistent with the observation that only the iodo compound is capable of oxidizing glutathione to the corresponding disulfide. Since a thiol function at the active site was capable of attacking an iodine bound to C-3, it seemed



reasonable to expect that same thiol to be in a position to attack the terminal CH_2 of **2**, because the same number of atoms would be involved in the bonding. The experiment with carboxyethyl disulfide described above was designed to show that if the active-site thiol is protected by disulfide formation as shown in Scheme III, then inactivation by **2** is prevented. The success of this experiment obviously provides only negative evidence that the thiol function is involved in the reaction with **2**. In view of all of the evidence, however, it seems reasonable to presume that the dissociable complex E \cdots **2** is the iminium ion formed by condensation of **2** with the essential lysine function, and that E-**2** is the covalent adduct formed by addition of an active-site thiol function to that iminium ion in a Michael fashion. The pH-rate profile for the inactivation reaction is not directly interpretable because of the considerable number of ionizable functional groups known to be near the active site¹⁸ and the uncertainty about their microscopic $\text{p}K_a$ values.

Since the adduct proposed to be the inhibited enzyme is hydrolyzable, attempts were made to measure the reversal of the inhibition reaction by two different methods. Repetitive chromatography on Sephadex G-25 at 25 °C gave a slow return of activity, since the hydrolysis reaction was occurring on the column where the inhibitor would be immediately separated from the reactivated protein. The rate constant for reactivation by this method is identical with that measured by incubation with mercaptoethanol, so that **2** would be trapped as hydrolysis occurred. The rate for the return of activity shows little dependence upon pH, with only a slightly lower rate at pH 7.0 than at 6.0 and 8.0.

At pH 7.0, the second-order rate constant for the reaction of **2** with the enzyme, $k_{\text{obsd}}^{\text{max}}/K_i^2 \approx 10^3 \text{ M}^{-1} \text{ s}^{-1}$, combined with the first-order rate constant for reactivation of $\sim 10^{-6} \text{ s}^{-1}$ gives an equilibrium constant of $\sim 10^9 \text{ M}^{-1}$ for adduct formation. (Approximate values are used because the reverse reaction was measured at 25 °C rather than 37 °C.) The binding constant

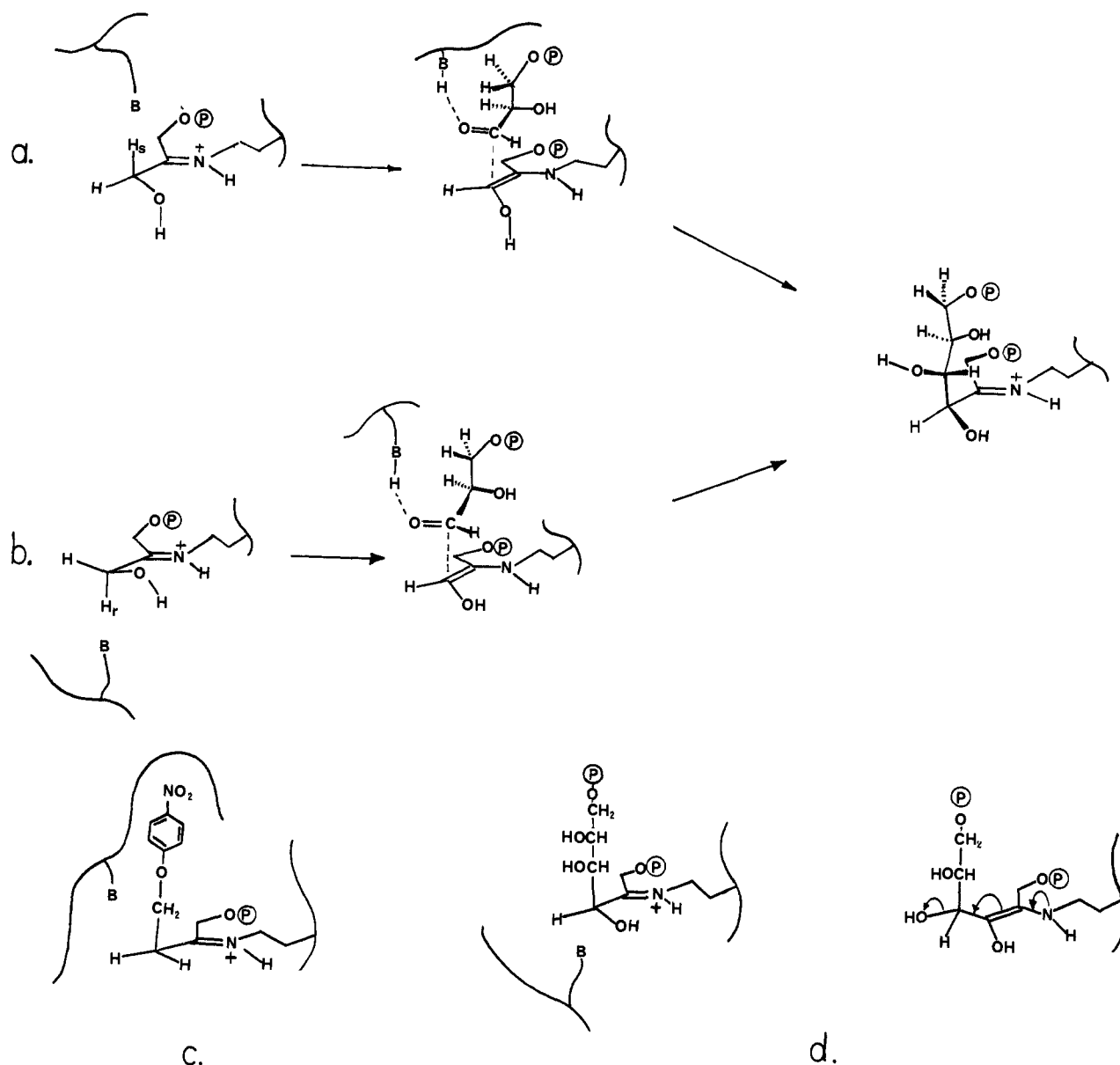


Figure 10. Route a shows the same-side replacement of a proton with glyceraldehyde 3-phosphate, whereas b shows the opposite-side analogue. Both lead to the same product, but route a, which requires some movement of B, is the path always chosen by evolution. The bound form of 1 shown in c does not undergo proton abstraction because the *p*-nitrophenyl group precludes the presence of the necessary base. This would not be the case for the opposite-side mechanism, which could possibly lead to enolization and dehydration of the fructose 1,6-bisphosphate as shown in d.

for **2** derives from the combination of two effects. There is the binding energy associated with the ketophosphate group, which is similar to other compounds containing these functions as demonstrated in Table I. There is also the additional binding energy associated with the presumed Michael reaction, for which there is an equilibrium constant of 10^4 favoring adduct formation.

As shown in Figure 10, the reaction catalyzed by aldolase is stereochemically cryptic³⁰ because the same product may be formed by removing the *pro-S* proton of DHAP and having glyceraldehyde 3-phosphate attack from the same side, or by removing the *pro-R* proton followed by attack on the opposite side. All of the aldolases that have been studied, including muscle aldolase, accomplish the reaction by having proton removal occur on the same side as aldehyde attack. Apparently there was considerable evolutionary pressure for selection of this same-side replacement, even though it requires movement of the proton abstracting base so that the aldehyde may take its place as shown in Figure 10.³¹ The accepted rationale for this behavior is that the selected mechanism allows a minimum

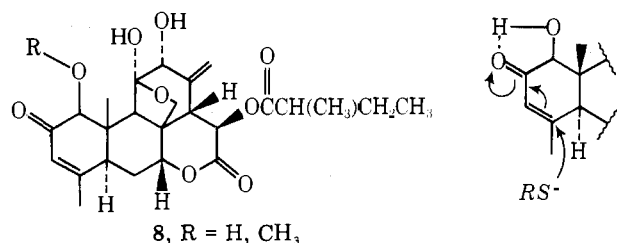
number of functional groups to be involved and proton recycling to occur.³⁰ The turnover number for aldolase is low enough, however, so that water could conceivably catalyze the proton transfers required for a two-base mechanism such as that shown in Figure 10b.

The data presented in Table I reveal that **1** is bound about as tightly as **4** and not much less well than DHAP. This suggests that the *p*-nitrophenoxy group is accommodated by the pocket normally occupied by C-4, -5, and -6 of fructose 1,6-bisphosphate. Since the presence of this large group precludes the presence of the proton-abstracting base, B, proton abstraction and subsequent elimination of *p*-nitrophenol are automatically prevented.

It is tempting to relate structural features of the active site of an enzyme solely to the ability to perform the appropriate catalytic task. However, the facts discussed above suggest that at least part of the evolutionary pressure that invariably generated same-side replacement arose because of the inability of these aldolases to catalyze elimination reactions. As shown in Figure 10d, if the base is available for proton abstraction at

C-3 when the fructose is in place, then it is possible for proton abstraction followed by elimination of hydroxide to occur. Aldolases that also catalyze dehydrations or epimerizations of sugars would be metabolically disastrous, and substantial evolutionary pressure would exist to prevent their selection. The fact that **1** is bound but not eliminated by aldolase may be a reflection of that pressure.

A number of plant metabolites have been identified which display significant cytotoxic and related antitumor activity.³² Certain combinations of functional groups appear frequently, such as the α -methylene lactones and the α -hydroxyenones. It has been proposed that this cytotoxicity arises because of the ability of these functions to react with enzyme thiol groups.^{33,34} The α -hydroxyenone function is proposed to be particularly reactive because of the hydrogen bonding assistance to nucleophilic attack on the enone as shown. Dehydroailanthinone (**8**), for example, loses antileukemic activity when the



α -hydroxy function is replaced with an α -methoxy function.³⁵ Because of the evidence cited above, an alternative explanation is reasonable. The hydroxy group may be phosphorylated after transport, and the molecule would then become an analogue of the type of inhibitor discussed in this study, making it an active site directed inhibitor of some kind. The lack of biological activity of the methyl derivative would be due to the fact that it cannot be phosphorylated.

Acknowledgments. We are grateful for financial support of this work by the Division of Research Development Administration of The University of Michigan and the American

Cancer Society through an institutional grant. Art Hanel performed some of the measurements described.

References and Notes

- (1) J. Wilde, W. Hunt, and D. J. Hupe, *J. Am. Chem. Soc.*, **99**, 3319 (1977).
- (2) R. H. Abeles and A. L. Maycock, *Acc. Chem. Res.*, **9**, 313 (1976).
- (3) B. L. Horecker, O. Tsolas, and C. Y. Lal, *Enzymes*, 3rd Ed., **7**, 213 (1972).
- (4) D. Portsmouth, A. C. Stoolmiller, and R. H. Abeles, *J. Biol. Chem.*, **242**, 2751 (1967).
- (5) (a) J. R. Butler, W. L. Alworth, and M. J. Nugent, *J. Am. Chem. Soc.*, **96**, 1617 (1975); (b) A. Vaz, J. R. Butler, and M. J. Nugent, *ibid.*, **97**, 5914 (1975).
- (6) D. J. Hupe, M. C. R. Kendall, and T. A. Spencer, *J. Am. Chem. Soc.*, **94**, 1254 (1972).
- (7) D. J. Hupe, M. C. R. Kendall, and T. A. Spencer, *J. Am. Chem. Soc.*, **95**, 2271 (1973).
- (8) (a) R. Neumann, R. Hevey, and R. H. Abeles, *J. Biol. Chem.*, **250**, 6362 (1975); (b) R. C. Hevey, J. Babson, A. L. Maycock, and R. H. Abeles, *J. Am. Chem. Soc.*, **95**, 6125 (1973).
- (9) R. Silverman and R. H. Abeles, *Biochemistry*, **16**, 5518 (1977).
- (10) T. L. Gresham and F. W. Shaver, U.S. Patent 2 449 991; *Chem. Abstr.*, **43**, 10531 (1949).
- (11) I. G. Per'kov, N. P. Komar, I. T. Polkovnichenko, and G. A. Popova, *Zh. Anal. Khim.*, **26**, 1037 (1971).
- (12) D. J. Hupe and D. Wu, *J. Am. Chem. Soc.*, **99**, 7653 (1977).
- (13) J. W. Donovan, *Biochemistry*, **3**, 67 (1964).
- (14) J. L. Jensen and H. Hashtroudi, *J. Org. Chem.*, **41**, 3299 (1976).
- (15) D. J. Hupe, M. C. R. Kendall, G. T. Sinner, and T. A. Spencer, *J. Am. Chem. Soc.*, **95**, 2260 (1973).
- (16) J. M. Wilson, R. J. Bayer, and D. J. Hupe, *J. Am. Chem. Soc.*, **99**, 7922 (1977).
- (17) H. P. Meloche, *Biochemistry*, **6**, 2273 (1967).
- (18) C. Y. Lai, N. Nakai, and D. Chang, *Science*, **183**, 1204 (1974).
- (19) F. C. Hartman, *Biochemistry*, **9**, 1776 (1970).
- (20) F. C. Hartman, *Biochemistry*, **9**, 1783 (1970).
- (21) J. Kowal, T. Cremona, and B. L. Horecker, *J. Biol. Chem.*, **240**, 2485 (1965).
- (22) I. A. Rose and E. L. O'Connell, *J. Biol. Chem.*, **244**, 126 (1969).
- (23) M. I. Page, *Angew. Chem., Int. Ed. Engl.*, **16**, 449 (1977).
- (24) R. P. Bell and M. A. D. Fluendy, *Trans. Faraday Soc.*, **59**, 1623 (1963).
- (25) E. T. Harper and M. L. Bender, *J. Am. Chem. Soc.*, **87**, 5625 (1965).
- (26) G. Lowe and R. F. Pratt, *Eur. J. Biochem.*, **66**, 95 (1976).
- (27) E. Grazi, C. Sivieri-Pecorari, R. Gagliano, and G. Trombetta, *Biochemistry*, **12**, 2583 (1973).
- (28) D. C. Wilton, *Biochem. J.*, **153**, 495 (1976).
- (29) C. T. Walsh and H. R. Kaback, *J. Biol. Chem.*, **248**, 5456 (1973).
- (30) K. R. Hanson and I. A. Rose, *Acc. Chem. Res.*, **8**, 1 (1975).
- (31) H. P. Meloche and J. P. Glusker, *Science*, **181**, 350 (1973).
- (32) G. R. Pettit, "Biosynthetic Products for Cancer Chemotherapy", Vol. 1, Plenum Press, New York, 1977.
- (33) S. M. Kupchan, *Pure Appl. Chem.*, **21**, 227 (1970).
- (34) E. Fujita and Y. Nagao, *Bioorg. Chem.*, **6**, 287 (1977).
- (35) S. M. Kupchan and J. A. Lacadle, *J. Org. Chem.*, **40**, 654 (1975).